

Sound in action: A squaraine derivative gels organic solvents upon application of ultrasound and addition

of a miniscule amount of SWCNTs considerably influences the self-assembly process (see scheme).

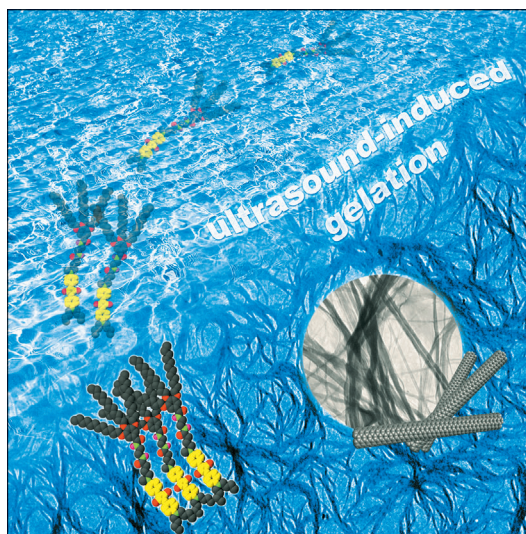
Hybrid Materials

J. M. Malicka, A. Sandeep, F. Monti, E. Bandini, M. Gazzano, C. Ranjith, V. K. Praveen, A. Ajayaghosh,* N. Armaroli** ■■■-■■■

Ultrasound Stimulated Nucleation and Growth of a Dye Assembly into Extended Gel Nanostructures 

Ultrasound-induced self-assembly and gelation ...

... is a hitherto unknown property of a squaraine derivative (**GA-SQ**). In their Full Paper on page ■ff., V. K. Praveen, A. Ajayaghosh, N. Armaroli et al. report detailed studies of the application of ultrasound to stimulate the nucleation and growth of extended nanostructures by altering the conditions for supersaturation. The influence of nanoscale substrates (SWCNTs) on the self-assembly of **GA-SQ** through a heterogeneous nucleation process is also demonstrated. This strategy could pave the way to the rational design of nanostructured composites by cheap and facile methods.



DOI: 10.1002/chem.201301539

Ultrasound Stimulated Nucleation and Growth of a Dye Assembly into Extended Gel Nanostructures

Joanna M. Malicka,^[a] Anjamkudy Sandeep,^[b] Filippo Monti,^[a] Elisa Bandini,^[a]
Massimo Gazzano,^[a] Choorikkat Ranjith,^[c] Vakayil K. Praveen,^{*,[a]}
Ayyappanpillai Ajayaghosh,^{*,[b]} and Nicola Armaroli^{*,[a]}

Abstract: A squaraine dye functionalized with a bulky trialkoxy phenyl moiety through a flexible diamide linkage (**GA-SQ**) capable of undergoing self-assembly has been synthesized and fully characterized. Rapid cooling of a hot solution of **GA-SQ** to 0°C results in self-assembled precipitates consisting of two types of nanostructures, rings and ill-defined short fibers. The application of ultrasound modifies the conditions for the supersaturation-mediated nucleation, generating only one kind of nuclei and prompting the formation of crystalline fibrous structures, inducing gelation of solvent mol-

ecules. The unique self-assembling behavior of **GA-SQ** under ultrasound stimulus has been investigated in detail by using absorption, emission, FT-IR, XRD, SEM, AFM and TEM techniques. These studies reveal a nucleation growth mechanism of the self-assembled material, an aspect rarely scrutinized in the area of sonication-induced gelation. Furthermore, in order to probe the effects of nanoscale sub-

strates on the sonication-induced self-assembly, a minuscule amount of single-walled carbon nanotubes was added, which leads to acceleration of the self-assembly through a heterogeneous nucleation process that ultimately affords a supramolecular gel with nanotape-like morphology. This study demonstrates that self-assembly of functional dyes can be judiciously manipulated by an external stimulus and can be further controlled by the addition of carbon nanotubes.

Keywords: gels · hybrid materials · nucleation and growth · sonication · squaraine

Introduction

Self-assembly of functional organic dyes to form extended nanostructures is a topic of current interest due to their possible applications in electronic and optoelectronic devices.^[1,2] Continuous research in this field has developed a number of methods to construct nanostructures with desired

shape, function, and uses.^[1–3] Typically, the methods employed in soft matter engineering are mild, in order to preserve the integrity of the resulting self-assembled materials in solution. In this regard, the discovery of sonication-induced formation of self-assembled nanostructures and consequent gelation of solvent molecules^[4] was rather unexpected, as the ultrasonic waves were believed to disrupt the self-assembly in solution.^[5] However, the interaction of ultrasonic sound waves with soft matter is known in medical diagnosis and transdermal drug delivery.^[6] Gels, akin to water, are excellent media to transmit ultrasound energy, with the advantage of being more viscous than water and thus easier to handle during the treatment. Another area of research in which ultrasound has contributed to substantial progress is the crystallization of molecules and materials.^[7] Ultrasound helps the primary nucleation process by modifying the conditions for supersaturation, thereby reducing the induction period between the attainment of supersaturation and the commencement of nucleation and crystallization. In addition, the excellent mixing conditions maintained by sonication-induced shockwaves have been shown to reduce the aggregation of crystals and allow the crystals to grow larger by controlling local nucleus population. In spite of the lessons from these totally different areas of research, supramolecular chemists overlooked these findings until Naota and Koori first observed the sol-to-gel transition of a dinuclear palladium complex that switches its conformation under the

[a] Dr. J. M. Malicka,* Dr. F. Monti, Dr. E. Bandini, Dr. M. Gazzano, Dr. V. K. Praveen, Dr. N. Armaroli
Istituto per la Sintesi Organica e la Fotoreattività
Consiglio Nazionale delle Ricerche (ISOF-CNR)
Via Gobetti 101, 40129 Bologna (Italy)
Fax: (+39)051-6399844
E-mail: nicola.armaroli@isof.cnr.it
praveen.karthikeyan@isof.cnr.it

[b] A. Sandeep,* Prof. Dr. A. Ajayaghosh
Photosciences and Photonics Group
Chemical Sciences and Technology Division
National Institute for Interdisciplinary Science and Technology
(NIIST), CSIR, 695019 Trivandrum (India)
Fax: (+91)471-2491712, 249018
E-mail: ajayaghosh62@gmail.com

[c] Dr. C. Ranjith
Dipartimento di Chimica Organica
Università degli Studi di Milano
Via Golgi 19, 20133 Milano (Italy)

[*] These authors contributed equally to this work.

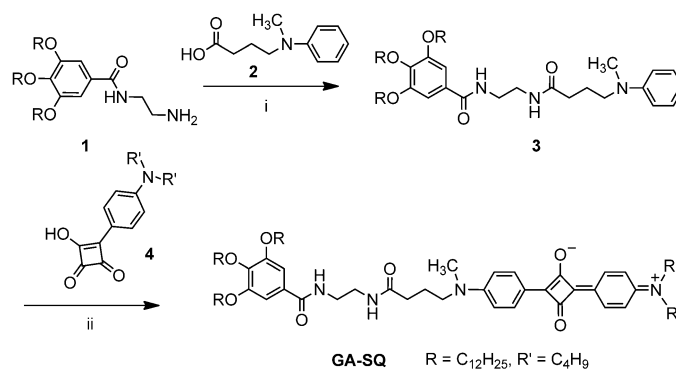
Supporting information for this article is available on the WWW under <http://dx.doi.org/10.1002/chem.201301539>.

influence of ultrasound to generate stabilizing intermolecular π -stacking interactions.^[4]

The last few years have witnessed a surge of activities in the field of sonication-induced gelation.^[8] A variety of molecules, such as metal complexes,^[9] peptides^[10,11] organic dyes,^[12] and hydrogen-bonded gelators^[10–13] have been utilized to accomplish sonogelation. Nevertheless, this approach has rarely been exploited for the development of functional gel-phase materials,^[9g,10d,11d,e] especially those composed of organic dyes.^[12] For instance, Yi, Huang, and co-workers have reported a family of cholesterol-appended naphthalimide molecules showing gelation^[12a,b] and morphological changes accompanied with gel-to-gel transition^[12c] under the influence of ultrasonic sound waves. Sonogelation of quinaclidone derivatives functionalized with urea^[12d] or cholesterol^[12e,f] moieties have been demonstrated by Zhang, Wang, and co-workers. Moreover, Jung et al., have observed that sonication could modulate the aggregation as well as gelation properties of a porphyrin–palladium(II) complex.^[12g]

Squaraines are an interesting class of polymethine-type dyes with resonance-stabilized zwitterionic structure. The unique combination of photostability and optical properties that span from the visible to the near-infrared region make squaraine dyes attractive for various applications in the areas of biology, chemistry, and material science.^[14] Aggregation properties of squaraines have been extensively studied in mixed solvents, organized media, and in the presence of metal ions.^[14b–e] However, there are only very few reports on the formation of extended supramolecular nanostructures of functional squaraine derivatives.^[15] The first example has come from the research group of Whitten, which reported the self-assembly of a cholesterol-tethered squaraine derivative, forming gel fiber networks incorporating organic solvents.^[15a] Some of us have reported a cation-induced expression of supramolecular chirality and morphological transition from spheres to helices of a chiral tripodal squaraine dye.^[15c,d] In another study, it was demonstrated that metal complexation promotes one-dimensional nanostructure formation of a tailor-made squaraine dye, yielding an enhancement of molar absorptivity due to the quantum confinement effect.^[15e] Evaporation-induced self-assembly of a simple squaraine dye into micrometer-long aligned nanowires has been reported by Zhang, Lee, and co-workers.^[15f] Very recently, Mayerhöffer and Würthner elucidated the thermodynamic and mechanistic aspects of a hydrogen-bonded assembly of a squaraine dye that forms extended fiber like aggregates.^[15b]

Construction of self-assembled structures of squaraine dyes continues to be important in the context of their renewed interest in light-energy harvesting and organic photovoltaics.^[16] Herein we report the unique properties of the squaraine derivative **GA-SQ** (Scheme 1), which forms ill-defined assembly under normal conditions, but forms extended nanostructures and gels upon application of ultrasound. With the help of spectroscopic and microscopic techniques, we demonstrate a nucleation and growth mechanism for the observed self-assembly, an aspect rarely studied in the area



Scheme 1. Synthesis of **GA-SQ** gelator. Reagents and conditions: i) BOP reagent, triethylamine, dry CH_2Cl_2 , RT, 3 h, 80%; ii) dry 2-propanol, tributyl orthoformate, 90 °C, 20 h, 37%.

of sonication-induced gelation of molecules.^[12b,13f] Furthermore, the addition of a minuscule amount of single-walled carbon nanotubes (SWCNTs) as a nanoscale substrate has been found to considerably influence the morphological properties of the **GA-SQ** sonogel by promoting a heterogeneous nucleation process.

Results and Discussion

The strategy adopted for the synthesis of squaraine gelator **GA-SQ** from compounds **1–4** is shown in Scheme 1. Compounds **1**, **2**, and **4** were prepared as per reported procedures.^[17] The preparation of compound **1** was achieved in three steps (see Scheme S1 in the Supporting Information). The first step was the reaction of methyl 3,4,5-trihydroxybenzoate with 1-bromododecane in the presence of K_2CO_3 .^[17a] The ester group of the resulting compound was hydrolyzed using KOH in ethanol to yield the corresponding carboxylic acid derivative.^[17a] The compound thus obtained was converted to the aminoethylbenzamide derivative **1** by reacting with excess ethylenediamine in the presence of benzotriazol-1-yloxytris(dimethylamino)phosphonium hexafluorophosphate (BOP), an amide coupling reagent.^[17b] Alkylation of *N*-methylaniline with ethyl 4-bromobutyrate in the presence of NaOAc and I_2 , followed by hydrolysis using 5% KOH, afforded *N*-methyl-*N*-(carboxypropyl)aniline (**2**; Scheme S2 in the Supporting Information).^[17c,d] 3-[4-(*N,N*-Dibutylamino)phenyl]-4-hydroxycyclobut-3-ene-1,2-dione (**4**) was prepared by reacting squaryl chloride^[17e] with *N,N*-dibutyl aniline (Scheme S3 in the Supporting Information).^[17f]

The amide-bond formation between aminoethylbenzamide derivative **1** and aniline **2** by using BOP in the presence of triethylamine gave **3** in 80% yield (Scheme 1). Reaction of **3** with the semisquaraine derivative **4** in a 1:1 stoichiometry, under reflux conditions in 2-propanol with tributyl orthoformate as the catalyst, resulted in the formation of the squaraine gelator **GA-SQ** (Scheme 1). The crude product first isolated by filtration was further purified by column

chromatography on neutral alumina and provided the pure product as a greenish blue solid in 37% yield.

The FT-IR spectrum of **GA-SQ** in CDCl_3 showed an intense band at 1589 cm^{-1} characteristic of pseudoaromatic squarate moiety (Figure S1 in the Supporting Information).^[17f] The amide carbonyl group of **GA-SQ** clearly discerned as a sharp band at 1660 cm^{-1} (Figure S1 in the Supporting Information). In the $^1\text{H NMR}$ spectrum of **GA-SQ** in CDCl_3 (Figure S2 in the Supporting Information), a singlet at $\delta = 3.04\text{ ppm}$ corresponds to the resonance of $-\text{NCH}_3$ protons. The signal at $\delta = 3.42\text{ ppm}$ is ascribed to the methylene protons of $-\text{CH}_2\text{NCH}_3$ and $-\text{CH}_2\text{NCH}_2-$, the resonance of which overlaps to appear as a multiplet. The signals at $\delta = 6.65, 6.70, 8.24,$ and 8.30 ppm are assigned to the protons of the diphenyl squaraine unit. The peak at $\delta = 7.08\text{ ppm}$ is attributed to the aromatic protons of the alkoxy-substituted gallic acid moiety. $^{13}\text{C NMR}$ (Figure S3 in the Supporting Information) and gradient heteronuclear single quantum correlation (gHSQC) (Figure S4 in the Supporting Information) spectra in CDCl_3 are in agreement with the structure of **GA-SQ**. The MALDI-TOF mass spectrum exhibits the 1175.27 [M]^+ ion peak along with 1197.92 [M+Na]^+ and 1214.37 [M+K]^+ peaks (Figure S5 in the Supporting Information). The absorption and emission spectra of **GA-SQ** in chloroform display a single band with the λ_{max} at 635 and 650 nm respectively with a relatively small Stokes shift $\Delta\nu_{\text{st}} = 412\text{ cm}^{-1}$ (Figure S6 in the Supporting Information). These optical features are very similar to the standard squaraine dyes derived from the reaction of squaric acid with *N,N*-dialkyl anilines.^[17f]

Gel formation is normally obtained by heating a required amount of gelator in a suitable solvent and subsequent cooling of the resultant homogenous solution either to room temperature or below.^[18a,b] The driving force for the formation of gel nanostructures is considered to be a supersaturation-mediated nucleation and growth.^[18] The gelator **GA-SQ**,^[19] owing to the presence of hydrophobic dodecyl chains, zwitterionic squaraine dye moiety, and amide functional groups, exhibits a multifaceted solubility character. In relatively polar solvents like CHCl_3 , CH_2Cl_2 , and THF **GA-SQ** is easily soluble and therefore, unsuitable for gelation studies. In aliphatic and aromatic solvents it is either insoluble or becomes soluble by heating at high temperature, but precipitates quickly on cooling. Interestingly, in protic polar solvents, such as aliphatic alcohols, **GA-SQ** becomes soluble at high temperatures, while upon cooling it exhibits two types of behavior. When a solution of **GA-SQ** in *n*-butanol is heated to 70°C and then let spontaneously cool down to room temperature, no apparent changes were observed. However, on rapid cooling to 0°C by inserting the sample in an ice bath, **GA-SQ** forms aggregates and the process is accompanied by a color change of the solution from cyan to dark violet (Figure 1 inset and Figure S7 in the Supporting Information). In order to visualize the morphology of these aggregates we carried out detailed electron microscopic studies. The aggregates of **GA-SQ** were cast on freshly cleaved mica and carbon-coated copper grids, air-dried, and

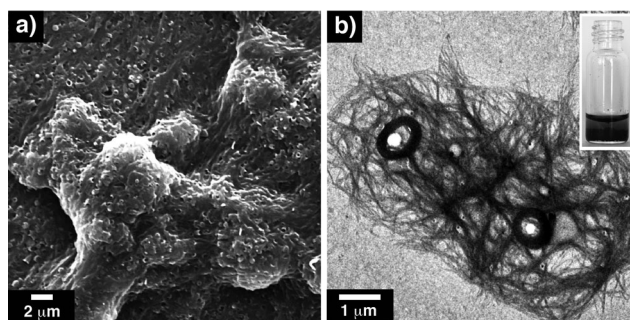


Figure 1. a) SEM and b) TEM images of **GA-SQ** self-assembled aggregates obtained by rapid cooling of a hot *n*-butanol solution (4 mM) to 0°C . The inset shows the photograph of the corresponding self-assembled precipitates formed in *n*-butanol, for a color picture see Figure S7 in the Supporting Information.

imaged by scanning electron microscopy (SEM) and transmission electron microscopy (TEM), respectively. SEM images show the formation of nanorings and ill-defined fibrous structures (Figure 1a). TEM analysis confirms that the aggregates entail nanorings surrounded by networks of short fibers that are a few micrometers in length (Figure 1b).

Even though the aggregates of **GA-SQ** failed to entrap solvent molecules and did not lead to gelation, the presence of polymorphic nanostructures was quite encouraging. Previous studies have demonstrated that regulating the formation of nuclei, its distribution and growth at the early stages of the self-assembling process would modify the kinetic pathways of supramolecular gel formation and consequent macroscopic properties.^[18b-d] In this regard, application of ultrasound has gained a lot of attention. Ultrasound is known to stimulate the primary nucleation process at a lower supersaturation level, which otherwise would not occur with other methods.^[7,8] Sonication also helps to break the seeds and disperse it uniformly in solution. In addition, the cavitation and streaming effect of the ultrasound waves ensure the bulk-phase mass transfer of solute to the surface of growing crystal, thereby promoting the secondary nucleation process. Based on this knowledge, we speculated that the application of ultrasound to a solution of **GA-SQ** might enhance the formation and growth of nuclei responsible for the formation of nanorings and fibers, by altering the condition for supersaturation. If the secondary nucleation process in the edges or sides of the developing nanostructure created permanent junction zones, an interconnected network structure capable of trapping solvent molecules by capillary force and van der Waals interactions might eventually arise.

To examine this possibility, detailed studies on the aggregation and gelation were carried out. Homogeneous solutions of various concentrations of **GA-SQ** in *n*-butanol were prepared at 70°C and then subjected to ultrasonication for 2 min (0.23 W cm^{-2} , 37 kHz) in a bath maintained at room temperature. As a control experiment, another batch of the same solutions was cooled to room temperature without applying sonication. In the lower concentration region (0.01–0.5 mM), the solutions cooled to room temperature in the

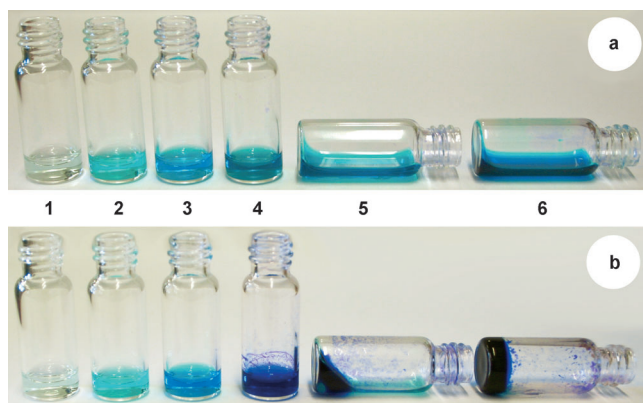


Figure 2. Photographs of the **GA-SQ** solutions in *n*-butanol cooled to room temperature a) in absence and b) presence of ultrasonic irradiation. Numbers correspond to the following concentration: 1=0.01 mM, 2=0.1 mM, 3=0.5 mM, 4=1 mM, 5=2 mM and 6=4 mM.

presence and absence of sonication show no difference (Figure 2). Interestingly, at a higher concentration range (1–4 mM), the sonication treatment gradually changed the color of the solutions from cyan to dark violet, whereas concentrated solutions cooled in the absence of sonication do not show any color variation (Figure 2). This finding underpins the key role of sonication, likely related to the modified conditions of supersaturation that promote the aggregation of molecules. Though at a concentration of 1 mM some aggregate formation is observed, the solution turned into a semi gel at a slightly higher concentration of 2 mM (Figure 2). A more stable gel is obtained at a concentration 4 mM, which prevented the flow of solvent upon tilting the sample vial sidewise or upside down (Figure 2). Sonication-induced gelation is also observed in other aliphatic alcoholic solvents, such as ethanol and *n*-propanol, with slightly higher critical gelator concentrations of 4.5 and 4.25 mM, respectively.

Insight on aggregation and gelation process can be obtained from the characteristic absorption properties of the squaraine moiety that changes upon aggregation.^[14,15] However, the high extinction coefficient of squaraines ($\sim 10^5 \text{ M}^{-1} \text{ cm}^{-1}$) together with the high concentrations used for these studies (mM) make it challenging to apply this technique. To circumvent these difficulties and enable a reasonable analysis, we used a special type of demountable flow cuvette with adjustable path length (for details see the Experimental Section and Figure S8 in the Supporting Information). UV/Vis absorption spectra of the investigated samples are presented in Figure 3 and Figures S9 and S10 in the Supporting Information. In the case of samples not exposed to sonication, the absorption spectra show a sharp band with λ_{max} at 640 nm, characteristic of the monomeric squaraine dye; its intensity changes proportionally to the concentration (Figure S9a in the Supporting Information), as visible by the naked-eye observation (Figure 2a). In the case of sonicated samples, solutions in the range 0.01–0.5 mM do not undergo aggregation (Figure 2b), which is confirmed by ab-

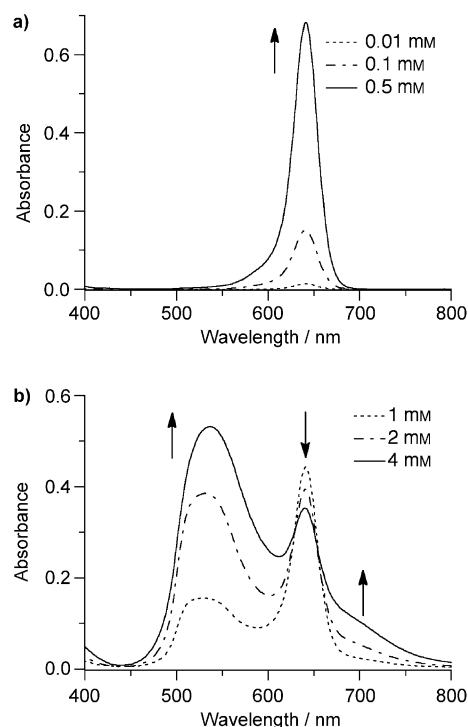


Figure 3. Absorption spectra of **GA-SQ** solutions after sonication a) lower and b) higher concentration region (path length, $l=0.05$ mm). Arrows indicates relative changes in absorption with increase in concentration.

sorption spectroscopy (Figure 3a and Figure S10 in the Supporting Information). However, for concentrations 1–4 mM, for which aggregation/gelation was observed (Figure 2b), absorption spectra reveal the presence of a new blue-shifted broad band with λ_{max} at 540 nm and a tail in the region between 675 and 800 nm, along with a reduced absorption of the monomeric squaraine at 640 nm. As the concentration increases, the band corresponding to the monomeric squaraine decreases in intensity with a concomitant increase in the absorption band at shorter wavelength with a tail in the lower energy region (Figure 3b). The observed broad spectrum suggests strong association of squaraine units in the aggregates of **GA-SQ** in a H-type fashion. The absorption features of self-assembled **GA-SQ** closely matches the spectral features of extended H-aggregates of squaraine amphiphiles and gelators.^[15a,20]

In light of the above results, it is important to gain insight into the morphology of the self-assembled **GA-SQ** obtained upon sonication. To this end, extensive microscopy studies were performed on *n*-butanol aggregates and gel cast on suitable substrates. SEM studies of a gel (4 mM) cast on freshly cleaved mica surface reveal the formation of entangled fibrous networks characteristic of self-assembled gels (Figure 4a). The width of the fibers varies from 50 to 400 nm and the length is extended to several micrometers. TEM micrographs of a diluted gel (2 mM) and aggregates (1 mM) cast on carbon-coated copper grids are shown in Figure 4b and Figure S11 in the Supporting Information, re-

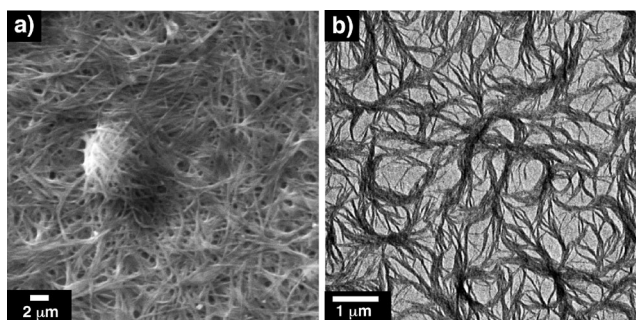


Figure 4. a) SEM and b) TEM images of sonication induced self-assembly of **GA-SQ** in *n*-butanol. The concentration used for SEM and TEM studies are 4 and 2 mM respectively.

spectively. The width and length of the thinnest fiber that can be distinguished is approximately 30 nm and few micrometers, respectively. The branching of fibers and the tangling of thin fibers to thicker fibrous structures can be also visualized from the TEM micrographs. The atomic force microscopy (AFM) studies on a dilute *n*-butanol gel (2 mM) cast on a freshly cleaved mica surface are also in agreement with the fiber-like morphology of the gel assembly, as observed with SEM and TEM. The AFM image of isolated fibers and its corresponding section analysis are shown in Figure S12 in the Supporting Information.

The morphological studies reveal that the formation of well-developed fibrillar structures of micrometer length and its entangling into network structures (Figure 4) are the key factors responsible for the gelation of **GA-SQ**. This result is in contrast with that obtained for the precipitated aggregates (heat and rapid cool method), for which the formation of thin fibers of few micrometers in length and ring-like structure are observed (Figure 1). The difference in morphology suggests that sonication substantially favors the formation of only one kind of nuclei by controlling the primary nucleation process and also helps the nuclei to grow further as one-dimensional fibers by facilitating the secondary nucleation events. The increased rates of these nucleation processes are a reflection of sonication-mediated efficient mass transfer from the bulk of the solution toward the growing nuclei to form the fibrous structure. However, in the case of rapid cooling, the slow rate of the primary and secondary nucleation processes possibly hampers the complete growth of the self-assembled nanostructures of **GA-SQ**, preventing further development into a network like morphology.

The above results prompted us to attempt a rationalization of the noncovalent interactions responsible for the self-assembly of **GA-SQ**. It is known that hydrogen bonding and van der Waals interactions play a crucial role in the self-assembly of molecules leading to gelation of solvents^[2b,e,18,21] and the best technique to probe this is FT-IR spectroscopy. A secondary amide group is characterized by three distinct IR absorptions corresponding to symmetric N–H stretch (amide A band), C=O stretch (amide I band) and a combination of the N–H deformation and of the C–N stretch (amide II band).^[22] These IR absorptions show change in

energy (frequency) when involved in hydrogen-bonding.^[22] The IR spectrum of **GA-SQ** in CDCl₃ (4 mM, Figure S13a in the Supporting Information) displays two bands at 3448 and 3342 cm⁻¹ that can be assigned as amide A bands. The aliphatic and aromatic amide carbonyl (amide I) appear as a single band at 1660 cm⁻¹ and the amide II band at 1527 cm⁻¹. By contrast, the IR spectrum of **GA-SQ** in the xerogel state exhibits a completely different behavior (Figure S13b in the Supporting Information). Thus, the amide A bands appear at 3301 and 3265 cm⁻¹, with a shift of 147 and 77 cm⁻¹ respectively. The amide I band splits into two bands displayed at 1650 and 1620 cm⁻¹, while the amide II shifts to 1539 cm⁻¹. The significant shifts of amide A and I bands to the lower frequency and the amide II band to the higher frequency region are clear indication of strong hydrogen bonding in the gel state.^[22] Another clear change is the shift of symmetric and asymmetric CH₂ vibrations of **GA-SQ** in gel state to 2849 and 2918 cm⁻¹ in comparison to those in CDCl₃, where they are observed at 2856 and 2928 cm⁻¹ respectively (Figure S14 in the Supporting Information). This observation implies that the alkyl chains of **GA-SQ** in the gel state are in all *trans* configuration and interdigitated.^[23] Similar observations were made in the case of **GA-SQ** self-assembled precipitates formed by rapid cooling to 0 °C (Figure S15 in the Supporting Information).

To investigate the involvement of the squaraine moiety in the observed aggregation properties of **GA-SQ**, temperature-dependent electronic absorption studies were per-

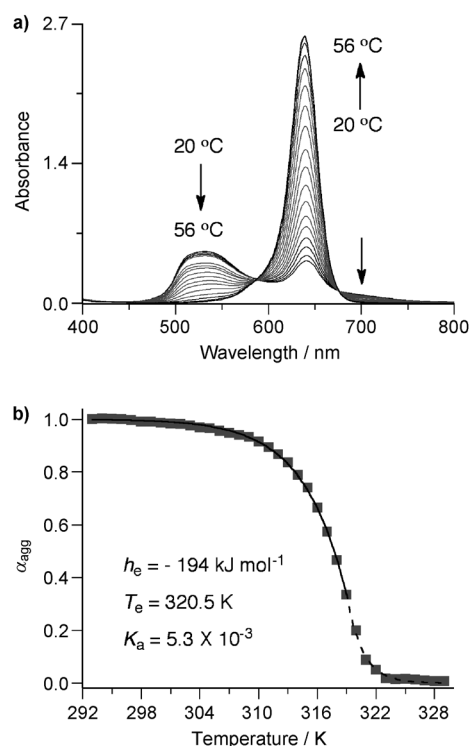


Figure 5. a) Temperature-dependent absorption spectra of **GA-SQ** *n*-butanol gel (2 mM) prepared by sonication (path length, $l=0.05$ mm). b) The plot of fraction of aggregates (α_{agg}) versus temperature fitted within elongation (solid line) and nucleation (dashed line) regimes.

formed, using the 2 mM *n*-butanol solution of **GA-SQ** that responds to sonication (Figure 5a). As the temperature is increased from 20 to 56 °C, the broad absorption in the wavelength region from 470 to 570 nm and the tail band observed between 675–800 nm exhibit a decrease in intensity with a concomitant increase in the absorption at 640 nm. These transitions are accompanied by two isosbestic points at 575 and 675 nm. The absorption spectra at higher temperatures are found to be similar to those in CHCl₃, in which **GA-SQ** mainly exists as a monomeric species. The absorption blue shift of the broad band with respect to the monomer suggests that the squaraine units are involved in H-type aggregation.^[15c-e,h,20b] On the other hand, the presence of the red-shifted tail extended to the near IR region suggests the contribution of an intermolecular charge-transfer interaction in the aggregate formation.^[20a] The formation of H-type aggregates was further confirmed by variable-temperature emission studies (Figure S16 in the Supporting Information). At low temperatures, the fluorescence of **GA-SQ** self-assembly is found to be completely quenched, which is a characteristic feature of H-type aggregation.^[15c-e,h] The emission band is restored at higher temperatures due to conversion of self-assembled **GA-SQ** into monomeric species.

The melting curve obtained from the temperature-dependent absorption studies is shown in Figure 5b. In order to demonstrate the involvement of nucleation and growth process in the observed self-assembly of **GA-SQ**, we have attempted to analyze the curve on the basis of the model proposed by van der Schoot, Schenning and Meijer.^[15h,24] According to this model, the fraction of aggregated molecules (α_{agg}) in the elongation and nucleation regime can be defined by the following Equations (1) and (2) respectively.

$$\alpha_{\text{agg}} = \alpha_{\text{SAT}} \left(1 - \exp \left[\frac{-h_c}{RT_c^2} (T - T_c) \right] \right) \quad (1)$$

$$\alpha_{\text{agg}} = K_a^{1/3} \left[\left(\frac{2}{3} K_a^{-1/3} - 1 \right) \frac{h_c}{RT_c^2} (T - T_c) \right] \quad (2)$$

The melting curve can be fitted with such elongation and nucleation functions (Figure 5b and Figure S17 in the Supporting Information). In the elongation regime the fit provides the molecular enthalpy released due to noncovalent interactions, h_c (−194 kJ mol^{−1}) and elongation temperature, T_c (320.5 K). The other parameters are the universal gas constant (R), absolute temperature (T) and α_{SAT} , a parameter necessary to equate $\alpha_{\text{agg}}/\alpha_{\text{SAT}}$ to unity. Fit of the nucleation regime gave the equilibrium constant K_a (5.3×10^{-3}) for the activation step at T_c . The satisfactory fit of the melting curve suggests the sonication-induced gelation involves a nucleation and elongation process.^[15h,19f,24]

To look closely into the packing of the molecules in the self-assembled structures of **GA-SQ** that are formed under different conditions, we have performed X-ray diffraction (XRD) studies. Figure 6a shows the XRD pattern of the **GA-SQ** xerogel film, which exhibits several well-resolved peaks characteristics of long-range crystalline ordering of the molecules. These peaks can be grouped and indexed in

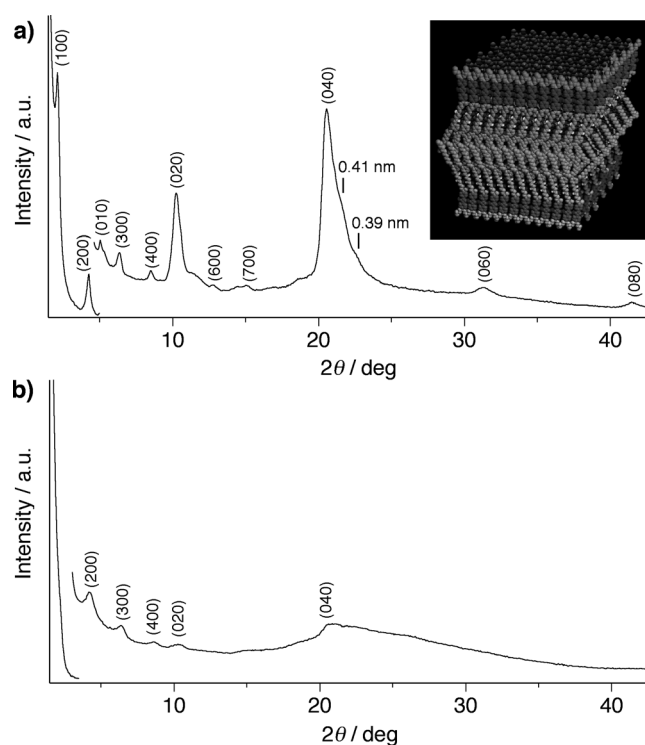


Figure 6. XRD patterns of **GA-SQ** a) xerogel film of *n*-butanol gel (4 mM) prepared by sonication and b) film of self-assembled aggregates obtained by rapid cooling of a hot *n*-butanol solution (4 mM) to 0 °C. Inset shows schematic representation of possible lamellar packing diagram of **GA-SQ** in the gel state.

two different sets based on the ratio of the d values. The first group shows reflections with d spacing of 4.17 (100), 2.08 (200), 1.39 (300), 1.04 (400), 0.69 (600), 0.59 nm (700). This implies that, in the gel state, molecules maintain a lamellar structure (Figure 6a inset) with the interlayer distance corresponding to 4.17 nm.^[23b,25] This distance is found to be in close match with optimized molecular length of **GA-SQ** (Figure S18 in the Supporting Information). A second group of peaks with d values of 1.74 (010), 0.86 (020), 0.43 (040), 0.29 (060) and 0.22 nm (080) indicate lateral packing of the molecules in the lamellar arrangement. The intense and broad reflection at $2\theta = 20.6^\circ$ (040) is found to consist of two shoulder peaks with d spacing values of 0.41 and 0.39 nm and can be ascribed to stacking of aromatic units assisted by secondary amide hydrogen bonding^[26] and crystalline packing of interdigitated alkyl chains respectively.^[23a,25d] Next, we have investigated the XRD of **GA-SQ** self-assembled precipitates formed by heating and rapid cooling to 0 °C. The diffractions peaks obtained from a thin film of precipitates are found to be less sharp in comparison to that of xerogel film (Figure 6b). Other noticeable differences are the absence of reflections corresponding to (100) and (010) planes and the presence of a diffuse halo in the wide-angle region due to distribution of reflections. The result of XRD studies suggests unregulated arrangement of molecules in the polymorphic nanostructures observed for self-assembled precipitates.

In principle, homogenous nucleation^[27] from the interior of a solution is difficult to occur.^[18b] Generally, all nucleation events are heterogeneous in nature and always involve some kinds of substrates. Heterogeneous nucleation effectively decreases the energy barrier for nucleation.^[18b] For example, in the case of crystallization of molecules, seeding of crystal enhances the crystallization process. Similarly, in the case of polymers^[28] and proteins,^[29] the presence of substrates, such as carbon nanotubes (CNTs) induce the crystallization process. CNTs are good choice as a nanoscale substrate also in supramolecular self-assembly, because of their propensity to facilitate the epitaxial growth of interacting molecules.^[30,31] Furthermore, the involvement of CNTs in the nucleation and growth process of a supramolecular soft material can give rise to interesting properties. With this objective, we decided to study the influence of SWCNTs on the sonication induced self-assembling behavior of **GA-SQ**.

A very small amount of SWCNTs (ca. 0.1 mg per 0.5 mL) was added to solutions of **GA-SQ** with concentration ranges from 0.01 to 4 mM. These samples were first heated at 70 °C and then subjected to sonication for 5 min. Control experiments were also performed by sonicating another batch of the solutions prepared without adding SWCNTs. After sonication, the 0.01 mM solution of **GA-SQ** with SWCNTs showed no color change, likewise the control sample. When the concentration of **GA-SQ** was raised to 0.1 mM, the solution with SWCNTs changed its color indicating an aggregation process; at a concentration of 0.5 mM the formation of dark violet aggregates was observed (Figure 7 a). In contrast, sonication was not found to affect the **GA-SQ** solution in the reference samples without SWCNTs (Figure 2b). This observation indicates that the synergic effect of sonication

and SWCNTs accelerates the aggregate formation of **GA-SQ** even at low concentrations. This underpins SWCNT-mediated heterogeneous nucleation and growth of **GA-SQ**.^[28,29,31] Interestingly, after sonication of 1 and 2 mM solutions with SWCNTs, formation of a semigel and a stable gel, respectively, were observed (Figure 7 a). In the absence of SWCNTs (see above) the semigel and gel of **GA-SQ** were observed for concentrations of 2 and 4 mM, respectively (Figure 2b). This means that the critical gelation concentration is reduced upon addition of a miniscule amount of SWCNTs. Apart from this, addition of SWCNTs is found to increase the stability of the composite gel as inferred from its gel melting temperature (T_{gel}) of 53 °C, whereas the pure **GA-SQ** gel showed a lower T_{gel} of 47 °C. Further evidence to the role of ultrasonic waves in the SWCNT-mediated heterogeneous nucleation of **GA-SQ** solutions was obtained from a control experiment in which the same solutions were heated to 70 °C and left cooled spontaneously till room temperature. Without application of ultrasound, none of them were able to undergo aggregation (Figure S19 in the Supporting Information).

The presence and involvement of SWCNTs in the observed self-assembly of **GA-SQ** can be easily probed by optical spectroscopy, through inspection of the peculiar absorption features of SWCNTs. Thus, the absorption spectrum of an aggregated solution of **GA-SQ** (0.5 mM), prepared by adding SWCNTs to a hot solution of **GA-SQ** followed by sonication, was recorded. The absorption spectrum shows the formation of the band corresponding to aggregated species of **GA-SQ** ($\lambda_{\text{max}} = 540$ nm, Figure 7 b). In addition, the spectrum clearly exhibits well-defined absorption bands in the near IR region, indicating van Hove singularities of dispersed SWCNTs (Figure 7 c).^[31,32] The absorptions corresponding to the electronic transitions of semiconducting nanotubes are observed between 750–900 nm (S_{22}) and 1000–1500 nm (S_{11}). The absorption features of metallic nanotubes are overlapped with the strong absorption of squaraines in the 400–700 nm region. The spectrum of SWCNTs dispersed in **GA-SQ** aggregates was then compared with that of SWCNTs dispersed in solution of sodium dodecylbenzenesulfonate (SDBS) in D_2O (Figure 7 c). Even though the effect of solvent cannot be completely ruled out, a clear redshift and broadening of the first-order semiconducting electronic transition S_{11} (1000–1500 nm) in the **GA-SQ** aggregates is observable, most likely due to electronic interactions of the aromatic units of **GA-SQ** with SWCNTs.^[32,33] Further evidence for the interaction between **GA-SQ** and SWCNTs is obtained from FT-IR studies. The aromatic C–H bending mode of **GA-SQ** observed between 700–900 cm^{-1} decreases its intensity in the presence of SWCNTs, indicating the strong interaction of aromatic moieties of **GA-SQ** with SWCNTs (Figure S20 in the Supporting Information).^[34]

After having observed the impact of SWCNTs on the aggregation and optical properties of the **GA-SQ** self-assembly, we investigated their effect on the nanoscale morphology. The TEM studies of **GA-SQ** aggregates formed at lower

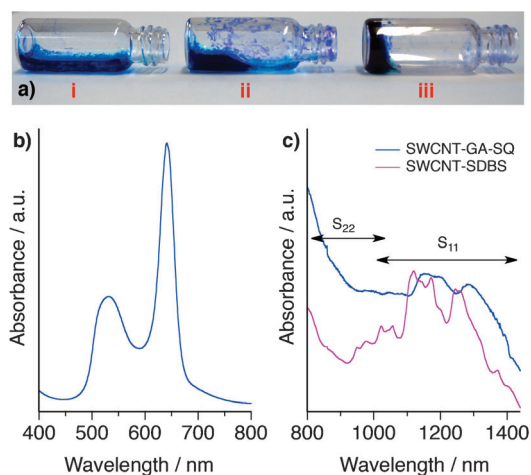


Figure 7. a) Photograph showing the changes of **GA-SQ** *n*-butanol solutions containing 0.1 mg of SWCNTs after ultrasound irradiation for 5 min. Numbers correspond to the following concentration: i=0.5, ii=1 and iii=2 mM. b) Absorption spectrum of sonication induced aggregates of **GA-SQ** formed in the presence of 0.1 mg of SWCNTs (*n*-butanol, *c*=0.5 mM, path length, *l*=0.5 mm). c) The absorption spectra of the same sample in the range 800–1400 nm showing van Hove singularities of SWCNTs. For a reference the absorption spectrum of SWCNTs dispersed in SDBS is also shown.

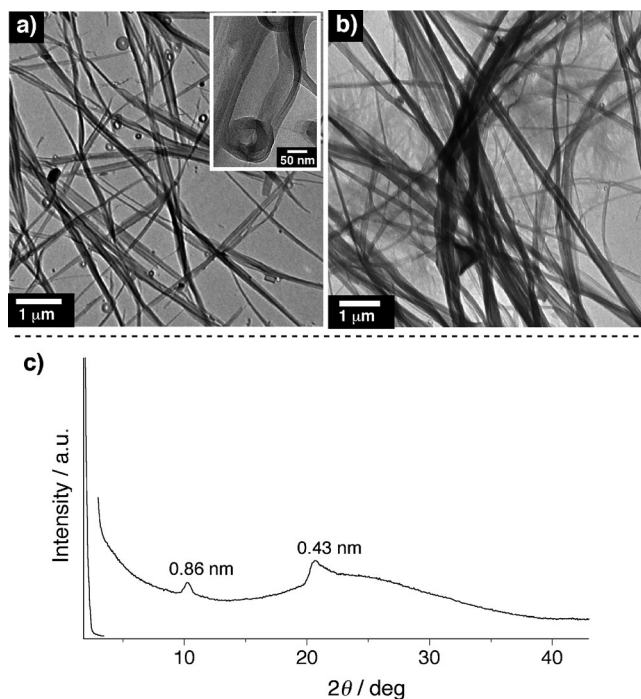


Figure 8. Effect of SWCNTs on the morphology of **GA-SQ** assembly. TEM images of **GA-SQ** a) aggregates (0.5 mM) and b) gel (2 mM). c) XRD patterns of the xerogel film (2 mM). The samples were prepared by adding a minuscule amount of SWCNTs to a hot solution of **GA-SQ** in *n*-butanol followed by sonication.

concentration (0.5 mM) showed the formation of micrometer long supramolecular nanotapes along with nanoring-like structures (Figure 8a). In some cases, the ring structures are found to open as part of nanotapes and their bundles (Figure 8a inset and Figure S21 in the Supporting Information), which indicate that they can be nanotape precursors. Interestingly, an almost complete transformation of nanorings is evident from the TEM micrograph of the **GA-SQ** gel (2 mM) that displays mainly nanotape-like morphology with bundles (Figure 8b). It should be noted that in the absence of SWCNTs, **GA-SQ** gel showed a rather different fiber-like morphology (Figure 4b). The substantial difference in morphology observed in the presence of very small amounts of SWCNTs indicates their influence in the self-assembling process of the squaraine molecule.

The observed difference in morphology is further confirmed by XRD studies. In contrast to the XRD profile of sonication-induced gel (Figure 6a), the gel formed in the presence of SWCNTs showed a XRD profile consisting of only few peaks (Figure 8c). It displayed two diffraction peaks at $2\theta = 20.68^\circ$ and 10.28° with *d* spacing of 0.43 and 0.86 nm respectively. The peak at $2\theta = 20.68^\circ$ is found to be broad and contains a small shoulder peak presumably due to the presence of reflection corresponding to stacking of aromatic units assisted by hydrogen bonding.^[26] The presence of a diffuse halo in the wide-angle region indicates alkyl chains are packed in a disordered manner.^[26c]

Conclusion

We have shown that a suitably designed squaraine dye equipped with dodecyloxy galloyl diamide unit (**GA-SQ**), undergoes ultrasound-triggered self-assembly and gelation, a hitherto unknown property for this class of molecules. The application of ultrasound is found to modify the conditions for the supersaturation-mediated nucleation and growth of **GA-SQ** self-assembly, which is apparent from the reluctance of the squaraine derivative to undergo aggregation by heating and slow cooling without sonication. On the other hand, self-assembly induced by just heating and rapid cooling to 0°C results in the formation of precipitates consisting of polymorphic nanostructures. Extended morphological analysis reveals that sonication prompts the formation of only one kind of nuclei leading to extended crystalline fibrous structures. Interestingly, the sonication of **GA-SQ** solutions containing a minuscule amount of SWCNTs promotes self-assembling in a lower concentration regime, at which mere sonication has no effect. The presence of the nanoscale substrate yields a nanotape-like morphology, which highlights the importance of nucleation events in shaping the final self-assembled material.^[18b-d,34] For the sonication induced gelation of **GA-SQ**, nucleation and growth is mainly determined by the crystalline packing of hydrophobic alkyl chains and hydrogen bonding, which promote the π - π stacking of the aromatic units. While, in the presence of SWCNTs, the adsorption of molecules on the heterogeneous surface, leads to a nucleation process assisted by π -stacking and hydrogen bonding. In this scenario, the establishment of a crystalline arrangement of the hydrophobic alkyl chains is more unlikely.

The strategy presented in this study paves the way to the rational design of nanostructured composites made of technologically relevant components such as functional dyes (squaraines) and carbon allotropes (fullerenes, CNTs, and graphene), with cheap and facile methods. The application of these intimately mixed composites as active materials in organic electronic devices for light-energy conversion and related application is a subject worth of investigation.

Experimental Section

Synthesis—general procedures: Unless otherwise stated, all starting materials and reagents were purchased from commercial suppliers and used without further purification. CH_2Cl_2 was dried over CaH_2 under N_2 and freshly distilled prior to use. Triethylamine was distilled in the presence of KOH and stored over KOH for further use. The reactions were monitored using thin layer chromatography on silica gel 60 F₂₅₄ (0.2 mm; Merck) or Al_2O_3 (0.2 mm; Merck). Visualization was accomplished using UV light or phosphomolybdic acid solution. Preparative column chromatography was performed on glass columns of different sizes hand packed with silica gel 60 (particle size 0.040–0.063 mm, Merck) or activated neutral Al_2O_3 (Sigma-Aldrich).

Synthesis—characterization techniques: NMR spectra were obtained on a Varian Mercury-400 spectrometer equipped with a 5 mm probe. Chemical shifts are reported in ppm using tetramethylsilane (TMS) ($\delta_{\text{H}} = 0$ ppm) or the solvent residual signal ($[\text{D}_6]\text{DMSO}$: $\delta_{\text{H}} = 2.49$ ppm, $\delta_{\text{C}} =$

39.50 ppm) (CDCl_3 ; $\delta_{\text{C}}=77.00$ ppm) as an internal reference. The resonance multiplicity is described as s (singlet), d (doublet), t (triplet), m (multiplet) and brs (broad singlet). IR spectra were recorded on a Perkin-Elmer Spectrum BX spectrometer using KBr sealed cell and plate for solution and film samples respectively. Matrix-assisted laser desorption ionization time-of-flight (MALDI-TOF) mass spectra were obtained on a Shimadzu AXIMA-CFR PLUS spectrometer using α -cyano-4-hydroxycinnamic acid as a matrix.

Synthesis of 3: Compounds **1** (1.79 g, 2.5 mmol), **2** (0.48 mg, 2.5 mmol), and BOP (1.1 g, 2.5 mmol) were dissolved in dry CH_2Cl_2 (50 mL). Triethylamine (0.39 mL, 2.75 mmol) was added and the reaction mixture stirred at room temperature for 4 h under N_2 atmosphere. The progress of the reaction was monitored using TLC. After the completion of the reaction, the organic layer was washed three times with brine, dried over anhydrous Na_2SO_4 , and filtered, and the filtrate was dried under reduced pressure. The residue was then subjected to column chromatography over silica gel (chloroform/methanol=8:2 v/v) to afford compound **3** as a white solid in 80% yield. FT-IR (CH_2Cl_2): $\nu_{\text{max}}=3444, 2926, 2854, 1658, 1600, 1582, 1494, 1468, 1379, 1331, 1114$ cm^{-1} ; $^1\text{H NMR}$ (400 MHz, CDCl_3 , TMS, 25°C): $\delta=0.88$ (m, 9H; $-\text{CH}_3$), 1.26–1.42 (m, 48H; $-\text{CH}_2-$), 1.45 (m, 6H; $-\text{OCH}_2\text{CH}_2\text{CH}_2-$), 1.71–1.81 (m, 6H; $-\text{OCH}_2\text{CH}_2-$), 1.90 (m, 2H; $-\text{NCH}_2\text{CH}_2\text{CH}_2\text{N}-$), 2.22 (t, $J=7.2$ Hz, 2H; $-\text{CH}_2\text{C}=\text{O}$), 2.85 (s, 3H; $-\text{NCH}_3$), 3.13 (t, $J=7.2$ Hz, 2H; $-\text{CH}_2\text{NCH}_3$), 3.46–3.54 (m, 4H; $-\text{NHCH}_2\text{CH}_2\text{NH}-$), 3.99 (m, 6H; $-\text{OCH}_2-$), 6.12 (brs 1H; $-\text{NH}$), 6.68 (m, 3H; phenyl-*H*), 7.00 (s, 2H; phenyl-*H*), 7.04 (brs, 1H; $-\text{NH}$), 7.19 ppm (m, 2H; phenyl-*H*); $^{13}\text{C NMR}$ (100 MHz, CDCl_3 , 25°C): $\delta=14.09, 22.68, 22.80, 26.07, 26.10, 29.35, 29.37, 29.41, 29.58, 29.64, 29.68, 29.70, 29.72, 29.73, 30.31, 31.91, 33.54, 38.05, 39.85, 41.55, 51.77, 69.17, 73.45, 105.47, 112.27, 116.35, 128.69, 129.17, 141.00, 149.32, 153.03, 168.01, 174.29$ ppm.

Synthesis of 3-(4-(*N,N*-Dibutylamino)phenyl)-4-hydroxy-cyclobut-3-ene-1,2-dione (4): *N,N*-Dibutyl aniline (4.2 g, 13.2 mmol) in dry benzene (50 mL) was added to a 100 mL round-bottomed flask containing squaryl chloride^[17e,f] (2.0 g, 13.2 mmol). After refluxing for 6 h, the reaction mixture was cooled and poured into crushed ice under stirring. The organic layer was separated, washed repeatedly with water (200 mL), dried over anhydrous Na_2SO_4 , and evaporated under vacuum. The residue dissolved in a mixture of acetic acid (50 mL), water (50 mL), and 2N HCl (4 mL) was refluxed for 2 h. After cooling to room temperature, the solid product was isolated by filtration, washed with diethyl ether and dried. FT-IR (KBr): $\nu_{\text{max}}=3451, 1755, 1595, 1419, 1362, 1191, 1020, 746, 674$ cm^{-1} ; $^1\text{H NMR}$ (400 MHz, $[\text{D}_6]\text{DMSO}$, 25°C): $\delta=0.91$ (t, $J=7.2$ Hz, 6H; $-\text{CH}_3$), 1.29 (m, 4H; $-\text{CH}_2-$), 1.48 (m, 4H; $-\text{CH}_2-$), 3.36 (t, $J=6.0$ Hz, 4H; $-\text{NCH}_2-$), 5.06 (brs 1H, $-\text{OH}$), 6.73–6.75 (d, 2H; phenyl-*H*), 7.83–7.86 ppm (d, 2H; phenyl-*H*); $^{13}\text{C NMR}$ (100 MHz, $[\text{D}_6]\text{DMSO}$, 25°C): $\delta=13.75, 19.50, 28.61, 50.12, 111.98, 128.00, 150.00, 173.14, 194.55$ ppm.

Synthesis of GA-SQ: Tributyl orthoformate (1 mL) was added to a 100 mL round-bottomed flask containing compounds **3** (0.45 g, 0.50 mmol), **4** (0.15 g, 0.50 mmol), and dry 2-propanol (50 mL). The reaction mixture was then stirred at 90°C for 20 h under N_2 . The progress of the reaction was monitored using TLC. After the completion of the reaction, the reaction mixture was cooled and filtered. The solid thus obtained was washed with 2-propanol until the filtrate become almost colorless. Column chromatography (chloroform/methanol=9:1 v/v) of the crude product over neutral Al_2O_3 gave the pure product in 37% yield. FT-IR (CDCl_3): $\nu_{\text{max}}=3348, 3342, 2928, 2855, 1660, 1589, 1527, 1390, 1361, 1177, 1110, 836, 790$ cm^{-1} ; $^1\text{H NMR}$ (400 MHz, CDCl_3 , TMS, 25°C): $\delta=0.87$ (t, $J=6.8$ Hz, 9H; $-\text{CH}_3$), 0.98 (t, $J=7.2$ Hz, 6H; $-\text{CH}_3$), 1.25 (m, 48H; $-\text{CH}_2-$), 1.41 (m, 10H; $-\text{OCH}_2\text{CH}_2\text{CH}_2-$ + $-\text{NCH}_2\text{CH}_2\text{CH}_2-$), 1.59–1.78 (m, 10H; $-\text{OCH}_2\text{CH}_2-$ + $-\text{NCH}_2\text{CH}_2-$), 1.93 (m, 2H; $-\text{NCH}_2\text{CH}_2\text{CH}_2\text{N}-$), 2.23 (t, $J=6.8$ Hz, 2H; $-\text{CH}_2\text{C}=\text{O}$), 3.04 (s, 3H; $-\text{NCH}_3$), 3.42 (m, 6H; $-\text{CH}_2\text{NCH}_3$ + $-\text{CH}_2\text{NCH}_2-$), 3.52 (m, 2H; $-\text{NHCH}_2-$), 3.59 (m, 2H; $-\text{NHCH}_2-$), 3.94 (m, 6H; $-\text{OCH}_2-$), 6.65 (d, $J=9.2$ Hz, 2H; phenyl-*H*), 6.70 (d, $J=9.2$ Hz, 2H; phenyl-*H*), 7.08 (s, 2H; phenyl-*H*), 7.21 (brs 1H; $-\text{NH}$), 7.74 (brs 1H; $-\text{NH}$), 8.24 (d, $J=9.2$ Hz, 2H; phenyl-*H*), 8.30 ppm (d, $J=9.2$ Hz, 2H; phenyl-*H*); $^{13}\text{C NMR}$ (100 MHz, CDCl_3 , 25°C): $\delta=13.84, 14.10, 20.20, 22.67, 22.93, 26.08, 26.10, 29.36, 29.43, 29.59, 29.66, 29.71, 29.74, 30.33, 31.91, 32.86, 38.48, 40.12, 41.24, 51.24, 51.68, 69.12, 73.42, 105.58, 112.26, 112.48, 119.27,$

119.65, 128.82, 132.76, 133.33, 140.88, 152.97, 153.75, 153.99, 168.06, 173.18, 183.42, 186.32, 187.46 ppm; MALDI-TOF-MS (matrix: α -cyano-4-hydroxycinnamic acid): m/z calcd for $\text{C}_{74}\text{H}_{118}\text{N}_4\text{O}_7$ $[M]^+$: 1174.90; found: 1175.27; m/z calcd for $[M+\text{Na}]^+$: 1197.89; found: 1197.92; m/z calcd $[M+\text{K}]^+$: 1214.00; found: 1214.37.

Optical measurements: Electronic absorption spectra were recorded on a Lambda 950 UV/VIS/NIR spectrophotometer (Perkin-Elmer). Photoluminescence spectra in chloroform were recorded on Edinburgh FLS920 spectrometer and temperature dependent photoluminescence was recorded on SPEX-Fluorolog F112X spectrofluorimeter using front face geometry. Optical studies in chloroform were carried out in a 1 cm quartz cuvette. Absorption studies of the aggregates/gel in *n*-butanol were carried out in a demountable flow cuvette (Figure S8 in the Supporting Information) with an option to vary path lengths using spacers of different thickness (FLAB-50-UV-01, GL Sciences, Japan). Fluorescence studies in the gel state were performed in a 1 mm quartz cuvette. All the solvents (CHCl_3 , *n*-butanol) are spectroscopic grade (99.8%) and were used as received.

Gelation studies: A weighed amount of the **GA-SQ** in an appropriate solvent (0.5 mL) was placed in a sealed glass vial (1 cm diameter) and dissolved by heating at 70°C. The solution was then subjected to sonication (0.23 Wcm^{-2} , 37 kHz, bath temperature 25°C, Elmasonic S10H) for 2 min. The sonication-induced gelation was considered successful if no sample flow was observed upon tilting the sample vial upside down.

To study the effect of carbon nanotubes, SWCNTs purchased from Unidym Inc (purified HiPco-SWCNTs, batch number: P2150) were used as received. A miniscule amount of SWCNTs (ca. 0.1 mg per 0.5 mL) was added quickly to a solution of **GA-SQ** in *n*-butanol prepared by heating at 70°C and the mixture was subjected to sonication for 5 min.

Scanning electron microscopy: SEM images were taken on a Zeiss EVO 18 cryo SEM Special Edn with variable pressure detector working at 20–30 kV after sputtering with gold. Samples were prepared by drop casting the aggregates (4 mm, rapid cooling method) and gel (4 mm, sonication) of **GA-SQ** in *n*-butanol on freshly cleaved mica substrate. It was kept for overnight to allow slow evaporation of the solvent and then further dried in a vacuum desiccator for 12 h.

Transmission electron microscopy: TEM imaging was performed on a JEOL-JEM0310 microscope with an accelerating voltage of 100 kV. Specimens were prepared by drop casting self-assembled materials of **GA-SQ** in *n*-butanol on carbon-coated copper grids (400 mesh) and dried under air. The dried sample was then desiccated for 12 h. The aggregates (rapid cooling method), aggregates (sonication) and gel (sonication) of **GA-SQ** were prepared using 4, 1 and 2 mM solutions respectively. The doped aggregates (0.5 mM) and gel (2 mM) of **GA-SQ** were prepared by adding a miniscule amount of SWCNTs to a hot solution of **GA-SQ** followed by sonication for 5 min.

Atomic force microscopy: AFM images were recorded under ambient conditions (298 K and 1 atm) by using a NTEGRA (NT-MDT) operating with a tapping mode regime. Micro-fabricated SiN cantilever tips (NSG10) with a resonance frequency of 299 kHz, curvature radius 10 nm and a force constant of 3.08–37.6 Nm^{-1} was used. AFM imaging was carried out using both height and magnitude profiles simultaneously. The section analysis was done offline. Samples for the imaging were prepared by drop casting diluted *n*-butanol sonogel of **GA-SQ** (2 mM) on freshly cleaved mica surface. The samples were first air dried and further under vacuum.

X-ray diffraction: For XRD, thin films of the samples were prepared by transferring self-assembled materials of **GA-SQ** in *n*-butanol into the cover slips and kept overnight for slow evaporation of the solvent. The X-ray diffractogram of the samples were recorded on a PANalytical X'Pert diffractometer equipped with a copper anode ($\lambda_{\text{mean}}=0.15418$ nm) and a fast X'Celerator detector collecting signals for 350 s in each step of 0.05°.

Acknowledgements

We acknowledge the European Commission for supporting V.K.P. (Marie Curie International Incoming Fellowship, GELBRID; PIIF-GA-2010-276574) and J.M.M. (Marie Curie Initial Training Network, FINELUMEN; PITN-GA-2008-215399) at CNR-ISOF. This work was supported by the Italian Ministry of Research (MIUR) and Consiglio Nazionale delle Ricerche (CNR) through PRIN 2010 INFOCHEM (contract no. CX2TLM), FIRB Futuro in Ricerca SUPRACARBON (contract no. RBFR10DAK6), MACOL PM. P04. 010, and Progetto Bandiera N-CHEM. J.M.M. further thanks Istituto di Studi Avanzati, University of Bologna, for the BRAINS-IN fellowship. A.S. is thankful to Council of Scientific and Industrial Research (CSIR), Government of India for a research fellowship. A.A. is grateful to the Department of Atomic Energy (DAE), Government of India, for a DAE-SRC Outstanding Researcher Award. The authors gratefully acknowledge Mr. C. K. Chandrakanth and Mr. Kiran Mohan of NIIST for SEM and TEM measurements, respectively.

- [1] For reviews, see: a) A. P. H. J. Schenning, E. W. Meijer, *Chem. Commun.* **2005**, 3245–3258; b) A. Ajayaghosh, V. K. Praveen, C. Vijayakumar, *Chem. Soc. Rev.* **2008**, 37, 109–122; c) T. Weil, T. Vosch, J. Hofkens, K. Peneva, K. Müllen, *Angew. Chem.* **2010**, *122*, 9252–9278; *Angew. Chem. Int. Ed.* **2010**, *49*, 9068–9093; d) F. Würthner, T. E. Kaiser, C. R. Saha-Möller, *Angew. Chem.* **2011**, *123*, 3436–3473; *Angew. Chem. Int. Ed.* **2011**, *50*, 3376–3410; e) Y. Yamamoto, *Sci. Technol. Adv. Mater.* **2012**, *13*, 033001; f) S. S. Babu, S. Prasanthkumar, A. Ajayaghosh, *Angew. Chem.* **2012**, *124*, 1800–1810; *Angew. Chem. Int. Ed.* **2012**, *51*, 1766–1776; g) E. Moulin, J. J. Cid, N. Giuseppone, *Adv. Mater.* **2013**, *25*, 477–487; h) J. D. Tovar, *Acc. Chem. Res.* **2013**, DOI: 10.1021/ar3002969.
- [2] For reviews, see: a) T. Ishi-i, S. Shinkai, *Top. Curr. Chem.* **2005**, 258, 119–160; b) S. Yagai, *J. Photochem. Photobiol. C* **2006**, *7*, 164–182; c) G. de La Torre, C. G. Claessens, T. Torres, *Chem. Commun.* **2007**, 2000–2015; d) Z. Chen, A. Lohr, C. R. Saha-Möller, F. Würthner, *Chem. Soc. Rev.* **2009**, *38*, 564–584; e) D. González-Rodríguez, A. P. H. J. Schenning, *Chem. Mater.* **2011**, *23*, 310–325; f) M. Li, S. Ishihara, Q. Ji, M. Akada, J. P. Hill, K. Ariga, *Sci. Technol. Adv. Mater.* **2012**, *13*, 053001; g) S. H. Kim, J. R. Parquette, *Nanoscale* **2012**, *4*, 6940–6947; h) M. B. Avinash, T. Govindaraju, *Adv. Mater.* **2012**, *24*, 3905–3922.
- [3] For different methods to prepare well-defined supramolecular nanostructures, see: a) L. Zang, Y. Che, J. S. Moore, *Acc. Chem. Res.* **2008**, *41*, 1596–1608; b) T. Yamamoto, T. Fukushima, T. Aida, *Adv. Polym. Sci.* **2008**, *220*, 1–27; c) A. Kaeser, A. P. H. J. Schenning, *Adv. Mater.* **2010**, *22*, 2985–2997; d) Y. S. Zhao, H. Fu, A. Peng, Y. Ma, Q. Liao, J. Yao, *Acc. Chem. Res.* **2010**, *43*, 409–418; e) K. Yoosaf, A. Llanes-Pallas, T. Marangoni, A. Belbakra, R. Marega, E. Botek, B. Champagne, D. Bonifazi, N. Armaroli, *Chem. Eur. J.* **2011**, *17*, 3262–3273; f) B.-K. An, J. Gierschner, S. Y. Park, *Acc. Chem. Res.* **2012**, *45*, 544–554.
- [4] T. Naota, H. Koori, *J. Am. Chem. Soc.* **2005**, *127*, 9324–9325.
- [5] J. M. J. Paulusse, D. J. M. van Beek, R. P. Sijbesma, *J. Am. Chem. Soc.* **2007**, *129*, 2392–2397.
- [6] For reviews, see: a) T. Watson, *Ultrasonics* **2008**, *48*, 321–329; b) M. R. Prausnitz, R. Langer, *Nat. Biotechnol.* **2008**, *26*, 1261–1268.
- [7] For reviews, see: a) L. H. Thompson, L. K. Doraiswamy, *Chem. Eng. Sci.* **2000**, *55*, 3085–3090; b) G. Rucroft, D. Hipkiss, T. Ly, N. Maxted, P. W. Cains, *Org. Process Res. Dev.* **2005**, *9*, 923–932; c) M. D. Luque de Castro, F. Priego-Capote, *Ultrason. Sonochem.* **2007**, *14*, 717–724.
- [8] For reviews, see: a) J. M. J. Paulusse, R. P. Sijbesma, *Angew. Chem.* **2006**, *118*, 2392–2396; *Angew. Chem. Int. Ed.* **2006**, *45*, 2334–2337; b) D. Bardelang, *Soft Matter* **2009**, *5*, 1969–1971; c) G. Cravotto, P. Cintas, *Chem. Soc. Rev.* **2009**, *38*, 2684–2697.
- [9] a) W. Weng, J. B. Beck, A. M. Jamieson, S. J. Rowan, *J. Am. Chem. Soc.* **2006**, *128*, 11663–11672; b) K. Isozaki, H. Takaya, T. Naota, *Angew. Chem.* **2007**, *119*, 2913–2915; *Angew. Chem. Int. Ed.* **2007**, *46*, 2855–2857; c) S. Zhang, S. Yang, J. Lan, Y. Tang, Y. Xue, J. You, *J. Am. Chem. Soc.* **2009**, *131*, 1689–1691; d) Y. He, Z. Bian, C. Kang, R. Jin, L. Gao, *New J. Chem.* **2009**, *33*, 2073–2080; e) L. Sambri, F. Cucinotta, G. De Paoli, S. Stagni, L. De Cola, *New J. Chem.* **2010**, *34*, 2093–2096; f) A. Kotal, T. K. Paira, S. Banerjee, T. K. Mandal, *Langmuir* **2010**, *26*, 6576–6582; g) N. Komiya, T. Muraoka, M. Iida, M. Miyanaga, K. Takahashi, T. Naota, *J. Am. Chem. Soc.* **2011**, *133*, 16054–16061.
- [10] a) Y. Li, T. Wang, M. Liu, *Tetrahedron* **2007**, *63*, 7468–7473; b) X. Wang, J. A. Kluge, G. G. Leisk, D. L. Kaplan, *Biomaterials* **2008**, *29*, 1054–1064; c) D. Bardelang, F. Camerel, J. C. Margeson, D. M. Leek, M. Schmutz, M. B. Zaman, K. Yu, D. V. Soldatov, R. Ziessel, C. I. Ratcliffe, J. A. Ripmeester, *J. Am. Chem. Soc.* **2008**, *130*, 3313–3315; d) D. Bardelang, M. B. Zaman, I. L. Moudrakovski, S. Pawsey, J. C. Margeson, D. Wang, X. Wu, J. A. Ripmeester, C. I. Ratcliffe, K. Yu, *Adv. Mater.* **2008**, *20*, 4517–4520; e) Y. Wang, C. Zhan, H. Fu, X. Li, X. Sheng, Y. Zhao, D. Xiao, Y. Ma, J. S. Ma, J. Yao, *Langmuir* **2008**, *24*, 7635–7638.
- [11] a) Z. Xie, A. Zhang, L. Ye, Z.-g. Feng, *Soft Matter* **2009**, *5*, 1474–1482; b) D. Ke, C. Zhan, A. D. Q. Li, J. Yao, *Angew. Chem.* **2011**, *123*, 3799–3803; *Angew. Chem. Int. Ed.* **2011**, *50*, 3715–3719; c) S. Maity, P. Kumar, D. Haldar, *Soft Matter* **2011**, *7*, 5239–5245; d) S. Maity, S. Sarkar, P. Jana, S. K. Maity, S. Bera, V. Mahalingam, D. Haldar, *Soft Matter* **2012**, *8*, 7960–7966; e) I. Maity, D. B. Rasale, A. K. Das, *Soft Matter* **2012**, *8*, 5301–5308; f) R. Afrasiabi, H.-B. Kraatz, *Chem. Eur. J.* **2013**, *19*, 1769–1777.
- [12] a) J. Wu, T. Yi, T. Shu, M. Yu, Z. Zhou, M. Xu, Y. Zhou, H. Zhang, J. Han, F. Li, C. Huang, *Angew. Chem.* **2008**, *120*, 1079–1083; *Angew. Chem. Int. Ed.* **2008**, *47*, 1063–1067; b) J. Wu, T. Yi, Q. Xia, Y. Zou, F. Liu, J. Dong, T. Shu, F. Li, C. Huang, *Chem. Eur. J.* **2009**, *15*, 6234–6243; c) X. Yu, Q. Liu, J. Wu, M. Zhang, X. Cao, S. Zhang, Q. Wang, L. Chen, T. Yi, *Chem. Eur. J.* **2010**, *16*, 9099–9106; d) C. Dou, C. Wang, H. Zhang, H. Gao, Y. Wang, *Chem. Eur. J.* **2010**, *16*, 10744–10751; e) C. Dou, D. Li, H. Gao, C. Wang, H. Zhang, Y. Wang, *Langmuir* **2010**, *26*, 2113–2118; f) C. Dou, D. Li, H. Zhang, H. Gao, J. Zhang, Y. Wang, *Sci. China Chem.* **2011**, *54*, 641–650; g) Y. Cho, J. H. Lee, J. Jaworski, S. Park, S. S. Lee, J. H. Jung, *New J. Chem.* **2012**, *36*, 32–35; h) Z.-X. Liu, Y. Feng, Z.-C. Yan, Y.-M. He, C.-Y. Liu, Q.-H. Fan, *Chem. Mater.* **2012**, *24*, 3751–3757; i) K. Liu, L. Meng, S. Mo, M. Zhang, Y. Mao, X. Cao, C. Huang, T. Yi, *J. Mater. Chem. C* **2013**, *23*, 1753–1762; j) H. Shigemitsu, I. Hisaki, H. Senga, D. Yasumiya, T. S. Thakur, A. Saeki, S. Seki, N. Tohnai, M. Miyata, *Chem. Asian J.* **2013**, *8*, 1372–1376.
- [13] a) C. Wang, D. Zhang, D. Zhu, *J. Am. Chem. Soc.* **2005**, *127*, 16372–16373; b) K. M. Anderson, G. M. Day, M. J. Paterson, P. Byrne, N. Clarke, J. W. Steed, *Angew. Chem.* **2008**, *120*, 1074–1078; *Angew. Chem. Int. Ed.* **2008**, *47*, 1058–1062; c) Y. Cao, L. M. Tang, Y. J. Wang, B. Y. Zhang, L. K. Jia, *Chem. Lett.* **2008**, *37*, 554–555; d) M. Yamanaka, H. Fujii, *J. Org. Chem.* **2009**, *74*, 5390–5394; e) Y.-Z. You, J.-J. Yan, Z.-Q. Yu, M.-M. Cui, C.-Y. Hong, B.-J. Qu, *J. Mater. Chem.* **2009**, *19*, 7656–7660; f) R.-Y. Wang, X.-Y. Liu, J.-L. Li, *Cryst. Growth Des.* **2009**, *9*, 3286–3291; g) C. Deng, R. Fang, Y. Guan, J. Jiang, C. Lin, L. Wang, *Chem. Commun.* **2012**, *48*, 7973–7975; h) T. Nakagawa, M. Amakatsu, K. Munenobu, H. Fujii, M. Yamanaka, *Chem. Lett.* **2013**, *42*, 229–231.
- [14] For reviews, see: a) K.-Y. Law, *Chem. Rev.* **1993**, *93*, 449–486; b) A. Ajayaghosh, *Acc. Chem. Res.* **2005**, *38*, 449–459; c) S. Sreejith, P. Carol, P. Chithra, A. Ajayaghosh, *J. Mater. Chem.* **2008**, *18*, 264–274; d) S. Yagi, H. Nakazumi, *Top. Heterocycl. Chem.* **2008**, *14*, 133–181; e) J. J. McEwen, K. J. Wallace, *Chem. Commun.* **2009**, 6339–6351; f) J. J. Gassensmith, J. M. Baumes, B. D. Smith, *Chem. Commun.* **2009**, 6329–6338; g) L. Beverina, P. Salice, *Eur. J. Org. Chem.* **2010**, 1207–1225; h) R. R. Avirah, D. T. Jayaram, N. Adarsh, D. Ramaiah, *Org. Biomol. Chem.* **2012**, *10*, 911–920; i) L. Hu, Z. Yan, H. Xu, *RSC Adv.* **2013**, *3*, 7667–7676; j) C. Qin, W.-Y. Wong, L. Han, *Chem. Asian J.* **2013**, DOI: 10.1002/asia.201300185.
- [15] a) C. Geiger, M. Stanescu, L. Chen, D. G. Whitten, *Langmuir* **1999**, *15*, 2241–2245; b) K. Jyothish, M. Hariharan, D. Ramaiah, *Chem. Eur. J.* **2007**, *13*, 5944–5951; c) A. Ajayaghosh, P. Chithra, R. Var-

- ghese, *Angew. Chem.* **2007**, *119*, 234–237; *Angew. Chem. Int. Ed.* **2007**, *46*, 230–233; d) P. Chithra, R. Varghese, K. P. Divya, A. Ajayaghosh, *Chem. Asian J.* **2008**, *3*, 1365–1373; e) A. Ajayaghosh, P. Chithra, R. Varghese, K. P. Divya, *Chem. Commun.* **2008**, 969–971; f) C. Zhang, X. Zhang, X. Zhang, X. Fan, J. Jie, J. C. Chang, C.-S. Lee, W. Zhang, S.-T. Lee, *Adv. Mater.* **2008**, *20*, 1716–1720; g) J. Wu, T. Yi, Y. Zou, Q. Xia, T. Shu, F. Liu, Y. Yang, F. Li, Z. Chen, Z. Zhou, C. Huang, *J. Mater. Chem.* **2009**, *19*, 3971–3978; h) U. Mayerhöffer, F. Würthner, *Chem. Sci.* **2012**, *3*, 1215–1220; i) Y. Ohsedo, M. Miyamoto, M. Oono, K. Shikii, A. Tanaka, *RSC Adv.* **2013**, *3*, 3844–3847; j) Z. Yan, S. Guang, H. Xu, X. Su, X. Ji, X. Liu, *RSC Adv.* **2013**, *3*, 8021–8027.
- [16] a) F. Silvestri, M. D. Irwin, L. Beverina, A. Facchetti, G. A. Pagani, T. J. Marks, *J. Am. Chem. Soc.* **2008**, *130*, 17640–17641; b) S. Wang, L. Hall, V. V. Diev, R. Haiges, G. Wei, X. Xiao, P. I. Djurovich, S. R. Forrest, M. E. Thompson, *Chem. Mater.* **2011**, *23*, 4789–4798; c) G. Chen, H. Sasabe, Z. Wang, X.-F. Wang, Z. Hong, Y. Yang, J. Kido, *Adv. Mater.* **2012**, *24*, 2768–2773; d) K. C. Deing, U. Mayerhöffer, F. Würthner, K. Meerholz, *Phys. Chem. Chem. Phys.* **2012**, *14*, 8328–8334.
- [17] a) S. Ghosh, X.-Q. Li, V. Stepanenko, F. Würthner, *Chem. Eur. J.* **2008**, *14*, 11343–11357; b) A. Dawn, N. Fujita, S. Haraguchi, K. Sada, S. Shinkai, *Chem. Commun.* **2009**, 2100–2102; c) H. Chen, W. G. Herkstroeter, J. Perlstein, K.-Y. Law, D. G. Whitten, *J. Phys. Chem.* **1994**, *98*, 5138–5146; d) M. Stanescu, H. Samha, J. Perlstein, D. G. Whitten, *Langmuir* **2000**, *16*, 275–281; e) R. C. De Selms, C. J. Fox, R. C. Riordan, *Tetrahedron Lett.* **1970**, *11*, 781–782; f) D. Keil, H. Hartmann, *Dyes Pigm.* **2001**, *49*, 161–179.
- [18] a) P. Terech, R. G. Weiss, *Chem. Rev.* **1997**, *97*, 3133–3160; b) J.-L. Li, X.-Y. Liu, *Adv. Funct. Mater.* **2010**, *20*, 3196–3216; c) P. A. Korevaar, S. J. George, A. J. Markvoort, M. M. J. Smulders, P. A. J. Hilbers, A. P. H. J. Schenning, T. F. A. De Greef, E. W. Meijer, *Nature* **2012**, *481*, 492–496; d) V. Stepanenko, X.-Q. Li, J. Gershberg, F. Würthner, *Chem. Eur. J.* **2013**, *19*, 4176–4183.
- [19] Trialkoxy galloyl diamide unit is an efficient self-assembly inducing segment, see: a) T. Kitahara, M. Shirakawa, S.-i. Kawano, U. Beginn, N. Fujita, S. Shinkai, *J. Am. Chem. Soc.* **2005**, *127*, 14980–14981; b) Y. Li, K. M.-C. Wong, A. Y.-Y. Tam, L. Wu, V. W.-W. Yam, *Chem. Eur. J.* **2010**, *16*, 8690–8698; c) A. Das, S. Ghosh, *Chem. Commun.* **2011**, *47*, 8922–8924; d) A. Jain, K. V. Rao, C. Kulkarni, A. George, S. J. George, *Chem. Commun.* **2012**, *48*, 1467–1469; e) S. Datta, S. Bhattacharya, *Chem. Commun.* **2012**, *48*, 877–879; f) F. Aparicio, F. García, L. Sánchez, *Chem. Eur. J.* **2013**, *19*, 3239–3248.
- [20] a) K.-Y. Law, *J. Phys. Chem.* **1988**, *92*, 4226–4231; b) K. Liang, K.-Y. Law, D. G. Whitten, *J. Phys. Chem.* **1994**, *98*, 13379–13384; c) H. Chen, M. S. Farahat, K.-Y. Law, D. G. Whitten, *J. Am. Chem. Soc.* **1996**, *118*, 2584–2594.
- [21] For reviews, see: a) F. Fages, F. Vögtle, M. Žinić, *Top. Curr. Chem.* **2005**, *256*, 77–131; b) A. Ajayaghosh, S. J. George, A. P. H. J. Schenning, *Top. Curr. Chem.* **2005**, *258*, 83–118; c) T. Seki, X. Lin, S. Yagai, *Asian J. Org. Chem.* **2013**, DOI: 10.1002/ajoc.201300025.
- [22] a) D. J. Skrovanek, S. E. Howe, P. C. Painter, M. M. Coleman, *Macromolecules* **1985**, *18*, 1676–1683; b) W. Herrebout, K. Clou, H. O. Desseyn, N. Bleton, *Spectrochim. Acta Part A* **2003**, *59*, 47–59; c) E. Jahnke, J. Weiss, S. Neuhaus, T. N. Hoheisel, H. Frauenrath, *Chem. Eur. J.* **2009**, *15*, 388–404.
- [23] a) N. Kameta, M. Masuda, H. Minamikawa, T. Shimizu, *Langmuir* **2007**, *23*, 4634–4641; b) T. Nakanishi, T. Michinobu, K. Yoshida, N. Shirahata, K. Ariga, H. Möhwald, D. G. Kurth, *Adv. Mater.* **2008**, *20*, 443–446; c) W. Jin, Y. Yamamoto, T. Fukushima, N. Ishii, J. Kim, K. Kato, M. Takata, T. Aida, *J. Am. Chem. Soc.* **2008**, *130*, 9434–9440.
- [24] a) P. Jonkheijm, P. van der Schoot, A. P. H. J. Schenning, E. W. Meijer, *Science* **2006**, *313*, 80–83; b) M. M. J. Smulders, A. P. H. J. Schenning, E. W. Meijer, *J. Am. Chem. Soc.* **2008**, *130*, 606–611.
- [25] a) L. A. Estroff, L. Leiserowitz, L. Addadi, S. Weiner, A. D. Hamilton, *Adv. Mater.* **2003**, *15*, 38–42; b) J.-H. Ryu, E. Lee, Y.-b. Lim, M. Lee, *J. Am. Chem. Soc.* **2007**, *129*, 4808–4814; c) S. Yagai, T. Kinoshita, M. Higashi, K. Kishikawa, T. Nakanishi, T. Karatsu, A. Kitamura, *J. Am. Chem. Soc.* **2007**, *129*, 13277–13287; d) H. Cao, Q. Yuan, X. Zhu, Y.-P. Zhao, M. Liu, *Langmuir* **2012**, *28*, 15410–15417.
- [26] a) F. D. Lewis, J.-S. Yang, C. L. Stern, *J. Am. Chem. Soc.* **1996**, *118*, 2772–2773; b) R. Abbel, R. van der Weegen, W. Pisula, M. Surin, P. Leclère, R. Lazzaroni, E. W. Meijer, A. P. H. J. Schenning, *Chem. Eur. J.* **2009**, *15*, 9737–9746; c) S. Diring, F. Camerel, B. Donnio, T. Dintzer, S. Toffanin, R. Capelli, M. Muccini, R. Ziessel, *J. Am. Chem. Soc.* **2009**, *131*, 18177–18185.
- [27] a) D. Erdemir, A. Y. Lee, A. S. Myerson, *Acc. Chem. Res.* **2009**, *42*, 621–629; b) P. G. Vekilov, *Cryst. Growth Des.* **2010**, *10*, 5007–5019; c) K. Harano, T. Homma, Y. Niimi, M. Koshino, K. Suenaga, L. Leibler, E. Nakamura, *Nat. Mater.* **2012**, *11*, 877–881.
- [28] For a review, see: L. Li, B. Li, M. A. Hood, C. Y. Li, *Polymer* **2009**, *50*, 953–965.
- [29] a) S. Linse, C. Cabaleiro-Lago, W.-F. Xue, I. Lynch, S. Lindman, E. Thulin, S. E. Radford, K. A. Dawson, *Proc. Natl. Acad. Sci. USA* **2007**, *104*, 8691–8696; b) C. Thauvin, S. Rickling, P. Schultz, C. Céilia, S. Meunier, C. Mioskowski, *Nat. Nanotechnol.* **2008**, *3*, 743–748; c) P. Asanithi, E. Saridakis, L. Govada, I. Jurewicz, E. W. Brunner, R. Ponnusamy, J. A. S. Cleaver, A. B. Dalton, N. E. Chayen, R. P. Sear, *ACS Appl. Mater. Interfaces* **2009**, *1*, 1203–1210.
- [30] For reviews, see: a) S. Srinivasan, A. Ajayaghosh, in *Supramolecular Soft Matter: Applications in Materials and Organic Electronics* (Ed.: T. Nakanishi), Wiley, Hoboken, New Jersey, **2011**, pp. 381–406; b) T. Fukushima, T. Aida, *Chem. Eur. J.* **2007**, *13*, 5048–5058.
- [31] a) S. Srinivasan, S. S. Babu, V. K. Praveen, A. Ajayaghosh, *Angew. Chem.* **2008**, *120*, 5830–5833; *Angew. Chem. Int. Ed.* **2008**, *47*, 5746–5749; b) Z. Tan, S. Ohara, M. Naito, H. Abe, *Adv. Mater.* **2011**, *23*, 4053–4057; c) S. K. Samanta, K. S. Subrahmanyam, S. Bhattacharya, C. N. R. Rao, *Chem. Eur. J.* **2012**, *18*, 2890–2901; d) S. K. Mandal, T. Kar, D. Das, P. K. Das, *Chem. Commun.* **2012**, *48*, 1814–1816.
- [32] a) C. Backes, C. D. Schmidt, F. Hauke, C. Böttcher, A. Hirsch, *J. Am. Chem. Soc.* **2009**, *131*, 2172–2184; b) C. Backes, U. Mündloch, A. Ebel, F. Hauke, A. Hirsch, *Chem. Eur. J.* **2010**, *16*, 3314–3317; c) J. K. Sprafke, S. D. Stranks, J. H. Warner, R. J. Nicholas, H. L. Anderson, *Angew. Chem.* **2011**, *123*, 2361–2364; *Angew. Chem. Int. Ed.* **2011**, *50*, 2313–2316; d) C. Romero-Nieto, R. García, M. Á. Heranz, C. Ehli, M. Ruppert, A. Hirsch, D. M. Guldi, N. Martín, *J. Am. Chem. Soc.* **2012**, *134*, 9183–9192.
- [33] Squaraine dyes are known to interact with CNTs and graphene, see: a) K. Yanagi, K. Iakoubovskii, H. Matsui, H. Matsuzaki, H. Okamoto, Y. Miyata, Y. Maniwa, S. Kazaoui, N. Minami, H. Kataura, *J. Am. Chem. Soc.* **2007**, *129*, 4992–4997; b) R. Tsuchikawa, H.-Y. Ahn, S. Yao, K. D. Belfield, M. Ishigami, *J. Phys. Condens. Matter* **2011**, *23*, 202204; c) Y. Xu, A. Malkovskiy, Y. Pang, *Chem. Commun.* **2011**, *47*, 6662–6664.
- [34] a) J. Zhang, J. K. Lee, Y. Wu, R. W. Murray, *Nano Lett.* **2003**, *3*, 403–407; b) S. Srinivasan, V. K. Praveen, R. Philip, A. Ajayaghosh, *Angew. Chem.* **2008**, *120*, 5834–5838; *Angew. Chem. Int. Ed.* **2008**, *47*, 5750–5754.
- [35] For polymorphism in supramolecular gel, see: a) S. van der Laan, B. L. Feringa, R. M. Kellogg, J. van Esch, *Langmuir* **2002**, *18*, 7136–7140; b) S. S. Babu, H. Möhwald, T. Nakanishi, *Chem. Soc. Rev.* **2010**, *39*, 4021–4035; c) I. D. Tevis, L. C. Palmer, D. J. Herman, I. P. Murray, D. A. Stone, S. I. Stupp, *J. Am. Chem. Soc.* **2011**, *133*, 16486–16494; d) A. Gopal, R. Varghese, A. Ajayaghosh, *Chem. Asian J.* **2012**, *7*, 2061–2067.

Received: April 22, 2013
Published online: ■ ■ ■, 0000